

STUDY OF A WALL SOLAR CHIMNEY TO REMOVE AIR FROM THE TOP OF AN INDOOR ENVIRONMENT

Thales de Freitas Villas Bôas, thalesfvb@fei.edu.br

Centro Universitário FEI, São Bernardo do Campo, SP, Brasil, 09850-901

Felipe Person Malta, fperson.malta@gmail.com

Escola Politécnica, Universidade de São Paulo, São Paulo, SP, Brasil, 05580-900

José Luiz Furtado Gouveia, lula@superlimao.com.br

SuperLimão Studio, São Paulo, SP, Brasil, 05433-010

Cyro Albuquerque Neto, cyroan@fei.edu.br

Centro Universitário FEI, São Bernardo do Campo, SP, Brasil, 09850-901

Abstract. *Solar chimneys inserted into the walls of a building might be used to improve indoor ventilation. This type of device can be used in both warm and cold climates, by only making a few arrangements in configuration. The aim of this work is to study the possibility of not only extract air from the bottom of an indoor environment, but also the upper portion of it. This could be achieved by obstructing the chimney's section at a certain height, while implementing a second inlet, the upper one, which will drag air from the indoor. The results showed that the existence of an upper inlet, promotes an increase in chimney's total air flow at up 10% , making this arrangement a great alternative over conventional chimney layout or even a small one, dedicated only to recirculate the top of an indoor environment. It was also found, that the main responsible for the flow increase, is the obstruction gap dimension, where narrower gaps are better.*

Keywords: *Thermal Comfort, Solar Chimney, Solar Energy, Passive Ventilation, Natural Convection*

1. INTRODUCTION

In spite of the non-constant characteristic, solar energy is free, sustainable, and is becoming more attractive as devices can handle better with the power efficiency and still having its cost reduced, leading to a worldwide tendency. Solar chimneys are a simple and convenient solution for ventilation and thermal comfort, it's layout can be fitted into a wall or even the roof of a building (Tan and Wong, 2012, Ziskind et al., 2002, Mathur et al., 2006), yet producing a regular air flow that can in some situations overtake the simple act of using an open window or door to ventilate (Khedari et al., 2000). However, it's optimization is strongly dependent from both design, materials and geometrical aspects, a fact that is well known for many researchers (Khanal and Lei, 2011).

Chen et al. (2003) carried out experimental studies with different inclination angles and heights. The maximum air flow rate was obtained for a 45° angle, with a height of 1.5 m and 200 mm gap (2/15 gap-to-height ratio). A further comparison of both vertical and inclined layouts resulted in a 45% increase of airflow for the inclined layout, and although it was not found an optimum chimney depth, it was noticed that the airflow rate increased directly with greater chimney depths. However, it is known by Bouchair (1994) that this increase has some limitations, such as a back flow at the outlet of the chimney, which can drastically affect the air flow rate, consequently, it was found that the optimum gap-to-height ratio is about 1/10. Recent studies (Jing et al., 2015) covered larger gap-to-height ratios, identifying an optimum value of 1/2, in which the author states that “the existence of the optimum chimney gap is debatable” as sometimes this optimum ratio cannot be estimated by researchers.

The chimney's inclination angle is also questionable, Imran et al. (2015) detected the optimum angle as being 60-degree, and observed that in this condition, the total air flow was 20% higher if compared to a 45-degree situation. It was also tested the variation of gap, and the authors concluded that even with 150 mm of gap, there wasn't any back flow/reverse flow.

The chimney inlet geometry has also direct impact on the air flow, Bassiouny and Koura (2008) determined that the inlet has an optimum area, but the entire chimney air flow rate is still more sensitive to the gap dimension. Amori and Mohammed (2012) designed a chimney with both conventional and side inlets (bottom placed), and were able to imply that the side inlet performs better, giving a higher thermal efficiency.

In order to consider a temperature uniformity along the cavity (height direction), Awbi (1994) and Sandberg (1999) proved that it can only be applied on chimneys that have less or at about 1/10 gap-to-height ratio, otherwise, larger ratios could lead the flow to a situation of the already said outlet back flow, producing temperature fluctuations along the section.

Ong (2003) proposed a mathematical model of the solar chimney by considering conduction, convection and radiation heat transfers, and were able to observe analytically the increase of air flow rate with higher chimneys,

something that was also discussed by Gan (1998) in which studies, by meaning of numerical simulations, resulted in the prediction of some equations for the air flow rate, such as a square root law dependence for the height dimension.

The solar radiation can be associated with the air flow rate, this was accomplished by Bansal et al. (1993) in which mathematical models showed that with a collector area of 2.25 m² and a solar radiation of 200 W/m² and 1000 W/m², air flow corresponds to 140 m³/h and 330 m³/h, respectively. Bassiouny and Korah (2009) presented their mathematical correlations for the air flow rate, returning acceptable values in the range of solar radiation tested, 500 W/m² to 750 W/m². In a further research, Bansal et al. (2005) demonstrated with an experiment and mathematical background the viability of changing a not-in-use window into a chimney by only making a few arrangements in its design.

A theoretical and experimental analysis of the chimney was made by Sandberg and Moshfegh (1996a), in this case, it was studied the thermal behavior of the cavity when inserting photovoltaic panels inside it. The results pointed out the importance of radiation heat transfer between the inner walls of cavity. The same authors (1996b) experimented a rain protected outlet layout, which resulted in an air flow rate of approximately 6 times lower compared to the straight orientation. Asadi et al. (2016) analyzed the optimum chimney layout for a seven-story office building, in which chimneys were interconnected by floors. The authors reported that locating the chimney in east-southern part of the building is the best option, since the radiation is greater and consequently, the ventilation rates.

Malta et al. (2013) studied a chimney inserted into a container's wall, concluding that temperature increase is almost linear with height, and that the chimney works even with low heat fluxes. In a further study, Malta et al. (2014) plotted both velocity and temperature profiles for the container's chimney, and were able to estimate an expression for the air flow rate. In a sequence, Villas-Bôas et al. (2015) investigated the influence of some design parameters in total air flow rate, detecting an optimum inlet and outlet heights for this particular type of chimney.

From the literature reviewed, it is unknown any studies for the issue on removing air from the top of the indoor environment, only the bottom or at most the side bottom. Therefore, the present work aims the viability of this scenery, bringing a first approach and quantification. To achieve this goal, an experimental apparatus was careful built.

2. EXPERIMENT

The experimental system consists of the solar chimney, a heater and a system of flow visualization. The entire system is described in the following sections.

2.1 Solar chimney

The chimney studied has a rectangular cross section of 370 mm x 20 mm and a height of 2 m. The bottom inlet as well as the outlet have a rectangular shape of 370 mm x 50 mm, however, the upper inlet is 370 mm x 10 mm. The chimney's conception is based on aluminum, MDF (medium density fibreboard), expandable polystyrene and PMMA (polymethyl methacrylate) as illustrated in Fig. 1. PMMA is here used as a clear surface with the intention of visualize the flow inside the chimney, meanwhile, expandable polystyrene is used as an insulator, MDF for structural elements and the aluminum for the heat incidence region.

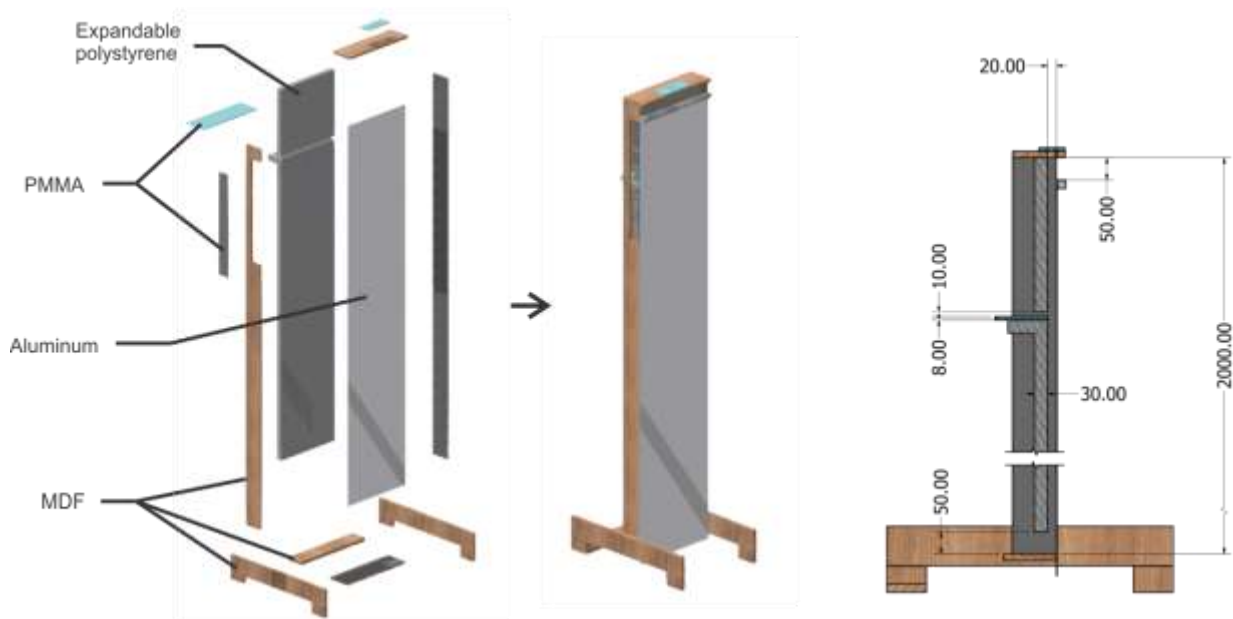


Figure 1. Chimney assembly and main dimensions in millimeters.

The chimney is placed vertically, through a custom support made of MDF, the gap-to-height ratio is given by a 20 mm gap and a 2000 mm height, resulting in 1/100.

2.2 Heater

Solar chimneys are generally exposed to the sunlight in real conditions, however, for test conditions, the incidence of sunlight might have abrupt fluctuations, which could compromise the entire work, based on comparisons. So it is highly important to have a constant incidence, by using an alternative to the sunlight. For this purpose, 4 ELBAC electrical resistances were mounted on a flat, metallic and reflective surface, being aimed to the frontal portion of the chimney. Each of the electrical resistances have 2.2 m height, \varnothing 9 mm and are capable of reaching 750 °C or 2000 W at 220 V.

2.3 Flow visualization

Flow visualization cannot quantify the flow, but it can clearly show the behavior of it, in other words, when applied to the chimney, it can show if there is any flow through the upper inlet. To accomplish that, a 400 W fog machine is used, this device can seed glycerin particles through the chimney, in which can be visualized with the assistance of a light sheet near the section of interest, in this case, the upper inlet section. The light sheet is created using a Laser, powered by a 3.7 V, 0.25 A source and providing visible light at a wavelength of 532 nm, in other words, a green colored laser, which is attached to optics such as cylindrical lenses. The laser is correctly positioned on the chimney, without interfering the flow neither the heating process.

A digital camera is placed outside the chimney, so it's field of view is the section of interest and its depth of field is basically the light sheet. The illumination adjustment is done by setting the camera parameters, including white balance (Auto), shutter speed (1/40), aperture (f5.0), ISO sensitivity (ISO 1600) as well as the focal length (40 mm), nevertheless, the image can later be adjusted with specific softwares.

2.4 Sensors and instrumentation

The chimney received its K-type thermocouples (accuracy of ± 2.0 °C) and an anemometer (Testo 405-V1, accuracy of 0.1 m/s + 5% of the measured value) as shown in Fig. 2, a compactDAQ from National Instruments was used for data acquisition, being processed through Signal Express software.

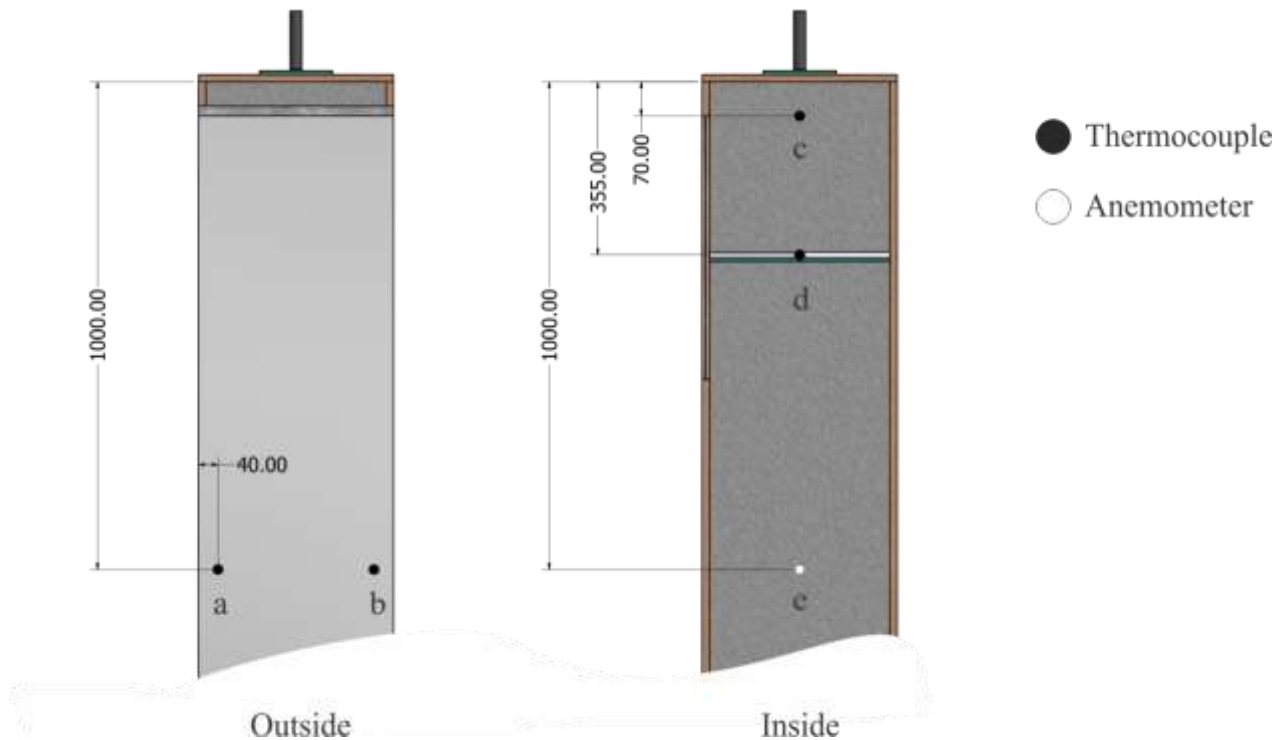


Figure 2. Measurement locations in millimeters.

3. MATHEMATICAL BACKGROUND

In order to estimate the air flow rates of both inlets and the outlet, some assumptions were made. For a first approach, it was used relations for the velocity profile from a previous work (Malta et al., 2014), as well as a linear correlation of heat and surface area receiving sun radiation. The heat loss through the insulator was not considered.

Firstly, the chimney can be energetically balanced into three different sceneries, as seen in Fig. 3, secondly, some ratios between the mass flow rates can be found, and finally, with some measurements of temperature and velocities, an estimated air flow for each boundary can be calculated.

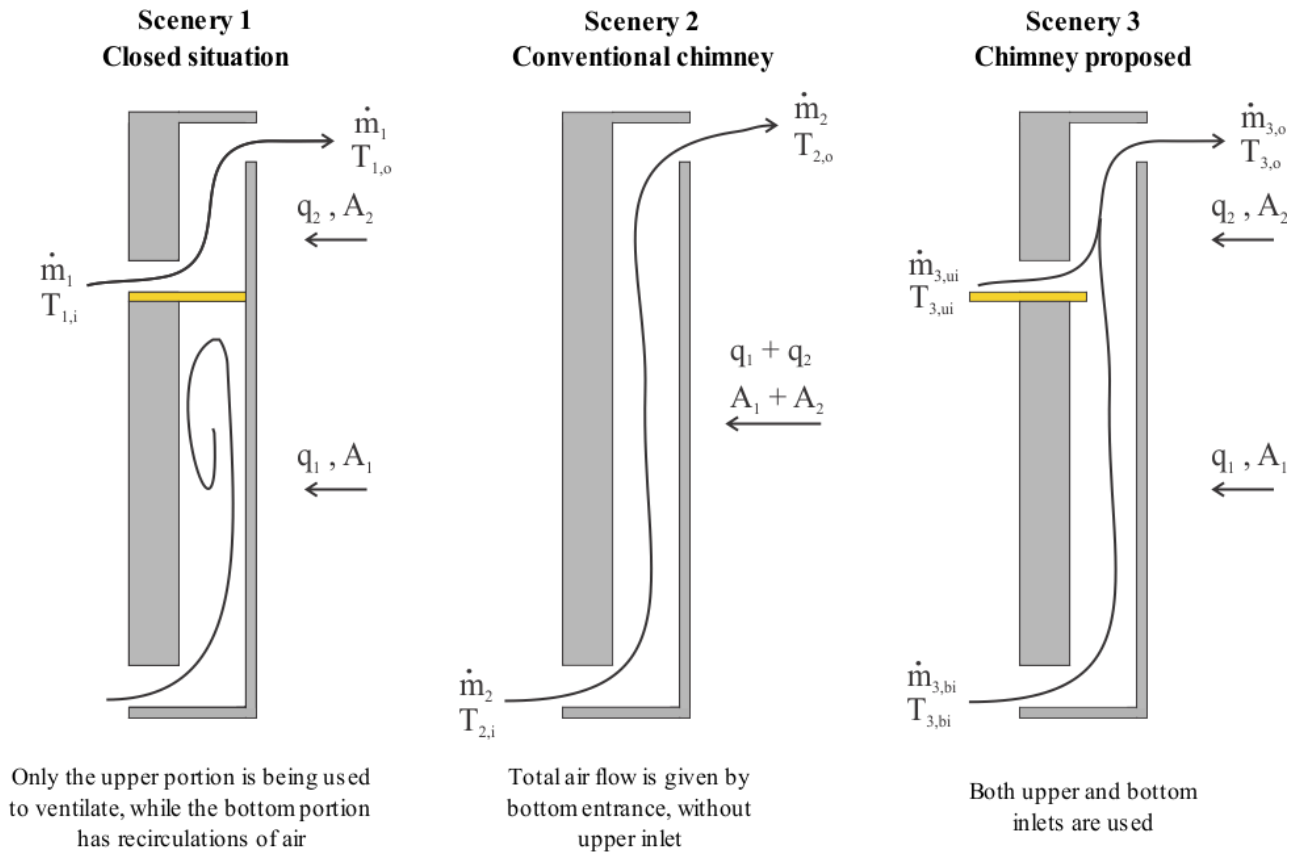


Figure 3. Different sceneries while operating a solar chimney.

3.1 Scenery 1 energy balance

Considering a closed section, the flow could only occur due to the heat at the upper portion of chimney (q_2 , W), while the lower portion (q_1 , W) would induce a recirculation. Applying an energy balance at the upper cavity formed, Eq. (1) is then obtained.

$$q_2 = \dot{m}_1 c_P (T_{1,o} - T_{1,i}) \quad (1)$$

where \dot{m}_1 is the mass flow rate ($\text{kg}\cdot\text{s}^{-1}$), c_P is the specific heat capacity at constant pressure ($\text{J}\cdot\text{kg}^{-1}\cdot\text{K}^{-1}$), $T_{1,i}$ and $T_{1,o}$ are the temperatures ($^{\circ}\text{C}$) at inlet and outlet, respectively.

3.2 Scenery 2 energy balance

In a conventional chimney, the heat flux is then the sum of each partial heat flux, and Eq. (2) is obtained.

$$q_1 + q_2 = \dot{m}_2 c_P (T_{2,o} - T_{2,i}) \quad (2)$$

where \dot{m}_2 is the mass flow rate ($\text{kg}\cdot\text{s}^{-1}$), $T_{2,i}$ and $T_{2,o}$ are the temperatures ($^{\circ}\text{C}$) at inlet and outlet, respectively.

3.3 Scenery 3 energy balance

The proposed chimney has both inlets, so the incident heat flux is also composed of both portions heat fluxes, therefore, resulting in Eq. (3).

$$q_1 + q_2 = \dot{m}_{3,o} c_p (T_{3,o} - T_{3,i}) \quad (3)$$

where $\dot{m}_{3,o}$ is the mass flow rate of outlet ($\text{kg}\cdot\text{s}^{-1}$), $T_{3,i}$ is the ambient temperature ($^{\circ}\text{C}$), here being considered equal for both inlets ($T_{3,a1} = T_{3,b1} = T_{3,i}$) since measurements indicated similar values, and $T_{3,o}$ is the outlet temperature ($^{\circ}\text{C}$).

3.4 Mass flow ratios

With all three equations, some correlations between the sceneries can be made. From Eq. (1) and Eq. (2) it is obtained Eq. (4).

$$\frac{\dot{m}_1}{\dot{m}_2} = \frac{A_2 (T_{2,o} - T_{2,i})}{A_1 + A_2 (T_{1,o} - T_{1,i})} \quad (4)$$

Eq. (2) and Eq. (3) reveals Eq. (5).

$$\frac{\dot{m}_2}{\dot{m}_{3,o}} = \frac{(T_{3,o} - T_{3,i})}{(T_{2,o} - T_{2,i})} \quad (5)$$

Lastly, Eq. (1) and Eq. (3) provides Eq. (6).

$$\frac{\dot{m}_1}{\dot{m}_{3,o}} = \frac{A_2 (T_{3,o} - T_{3,i})}{A_1 + A_2 (T_{1,o} - T_{1,i})} \quad (6)$$

where A_1 and A_2 are the solar radiation incidence areas for the lower portion and upper portion, respectively.

4. EXPERIMENTAL PROCEDURES

Some obstruction gaps and fluid expansions were tested, this was achieved by rotating the upper insulator towards the cavity, thus promoting a smooth cavity variation along the chimney's upper portion. This can be clarified by Fig. 4.

In a first part of the experiment, reference geometries were tested, that is, the closed situation (scenery 1) and the conventional chimney (scenery 2). In the second part, obstruction gaps (GAPo) were varied from 0 mm to 20 mm by increments of 5 mm, while the insulator gap (GAPi) varied from 10 mm to 20 mm with the same increment. Finally, the third part consisted on varying only the obstruction gap, by the same increments than before, but this time, with the insulator gap fixed at 20 mm.

Heater was turned on, and approached from chimney's frontal aluminum sheet. Data acquisition was initiated after thermocouples reach steady-state. The experiment consisted of a measuring part, where temperatures and velocities were observed and recorded during 15 seconds, as well as an image capturing part, where glycerin particles were seeded (after the measurements) at both inlets, one at a time, and captured with the digital camera.

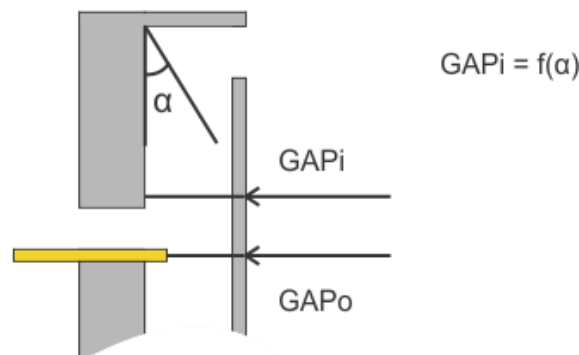


Figure 4. Insulator and obstruction gaps (GAPi and GAPo).

5. RESULTS AND DISCUSSION

The laboratory is placed at São Bernardo do Campo – São Paulo, with an atmospheric pressure of around 693 mmHg. The ambient temperature had little fluctuation during test, staying at 16.5 ± 0.06 °C (average \pm standard deviation).

In the beginning, the chimney didn't behave as expected, it was discovered later, that the proximity of the heater had a direct effect on the chimney's flow. The atmospheric air between the heater and the chimney have also suffered from buoyancy forces, and the small distance between them acted similarly as a cavity. This external flow, interfered in the chimney's outlet flow, hindering it.

In order to overcome this problem, it was added a piece of expandable polystyrene as a blocker for the external flow, thus reducing the interference. This modification had an enormous impact over the chimney's flow, which started to behave as intended.

When using the chimney as conventional layout (scenery 2), mass air flow resulted in $2.049 \text{ g}\cdot\text{s}^{-1}$ (\dot{m}_2), while using the chimney totally closed (scenery 1) resulted in a mass air flow (\dot{m}_1) of $0.441 \text{ g}\cdot\text{s}^{-1}$, in this scenery, only the upper inlet is used to remove air from room, this could be an arrangement to be used in conditions like toxic gas or heated gas removal.

For the proposed chimney (scenery 3), it is important to note that when $\text{GAP}_i < \text{GAP}_o$, fluid starts to hit the insulator surface instead of solely the obstruction plate, hence, vortexes are necessarily created, due to the directioning of fluid towards the upper inlet, something that was actually observed and it is totally prejudicial. That's the main reason for the chosen gaps in the second part of the experiment, where the insulator was always dephased by 5 mm from insulator and the expression $\text{GAP}_i = (\text{GAP}_o + 5 \text{ mm})$ was valid.

For greater differences between GAP_i and GAP_o , while $\text{GAP}_i > \text{GAP}_o$, it was noticed from a previous test (higher gap-to-height ratio) the existence of an increase of the vortexes creation tendency, until a limit where vortexes are complete developed. Those vortexes occur right above the upper inlet, affecting drastically the entering air flow. However, due to the maximum gap of 20 mm, it was not observed any consistent vortex with the tested geometries.

Flow visualization can be seen in Fig. 5 and Fig. 6, where both upper inlet (red colored smoke) and bottom inlet (green colored smoke) flows were captured and then merged with the assistance of an image software. Geometries are labeled as ratios, meaning "GAP_o/GAP_i" as a manner to refer to a specific configuration tested.

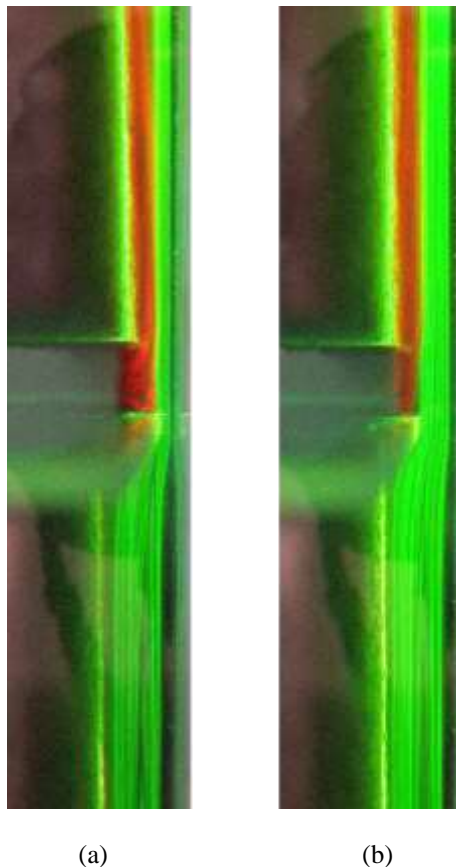


Figure 5. Flow visualization for 5/10 (a) and 10/15 (b) ratios of GAP_o/GAP_i.

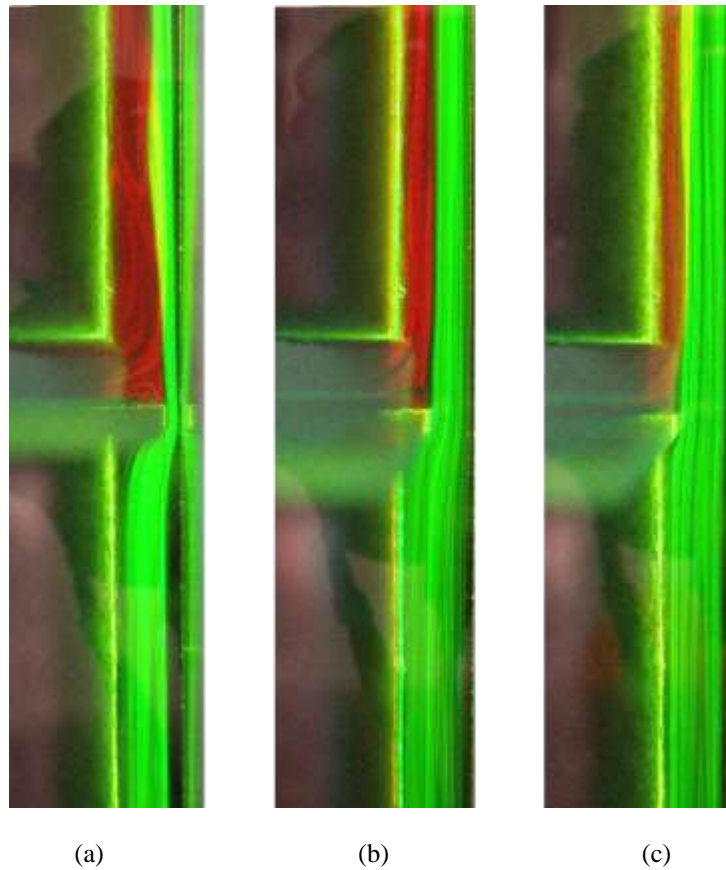


Figure 6. Flow visualization for 5/20 (a), 10/20 (b) and 15/20 (c) ratios of GAPo/GAPi.

Through Fig. 5 and Fig. 6, there's no doubt that the cavity acted as an air inlet, suctioning a great amount of air. It can also be seen, that the amount of air suctioned is highly influenced by GAPo, since lower GAPo's lead to an increase on upper inlet's air flow.

By Fig. 7 it is clearly that all tested geometry combinations induced an increase in total removed air flow, that means, the existence of the upper inlet, by itself, caused an increase in the chimney's overall performance. A simple opening in insulator (point 20/20) brought a 2.7% increase in total air flow compared to a conventional chimney layout.

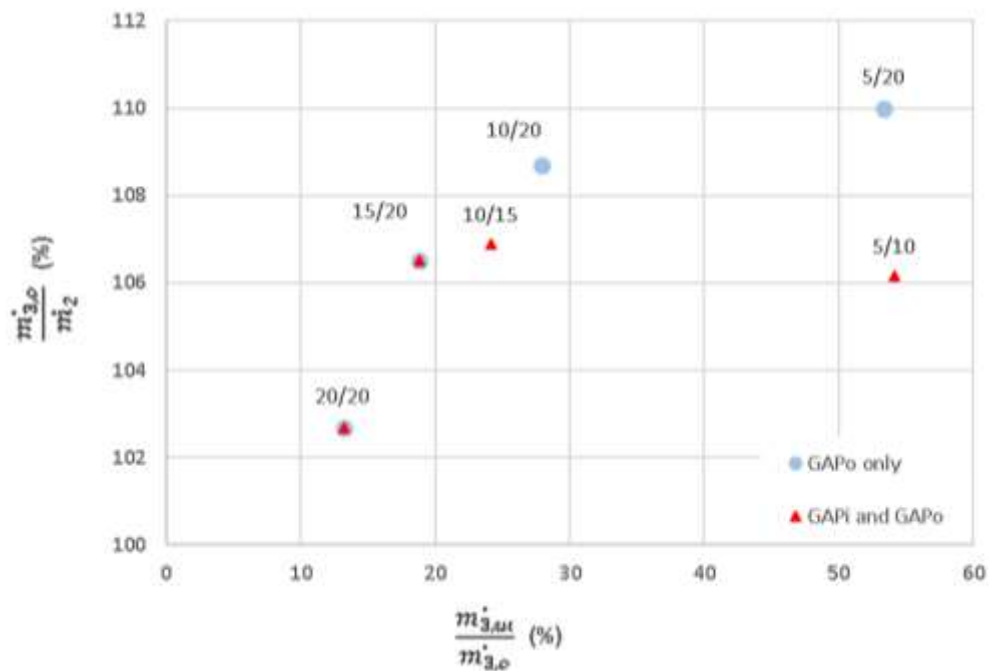


Figure 7. Increase of air flow over scenery 2 by upper inlet fraction, labels represent the ratio of GAPo/GAPi tested.

It can also be observed that the variation of GAPi had a negative effect over the total air flow removed from chimney, mainly due to a decrease in the upper inlet air flow. Nevertheless, it is worth to be highlighted the constructive complexity that a chimney with GAPi and α variations takes, which not only is less beneficial, but also has implementation issues.

By analyzing the increase in air flow over the closed situation (scenery 1) by doing a ratio between $\dot{m}_{3,ui}^*$ and $\dot{m}_{1,1}$, becomes clear that some configurations are capable of not only removing greater air flow over conventional chimney, but are also capable of remove greater air flow over a smaller chimney, arranged as scenery 1. This demonstrates that a chimney with upper and bottom inlets not only can be versatile, but it is also robust.

In all conditions tested, the temperature difference between outlet and inlets were almost the same, staying at $17.1 \pm 0.4^\circ\text{C}$ (average \pm standard deviation)., and among all, the best situation observed was with the GAPi fixed at 20 mm and GAPo at 5 mm, resulting in 10% air removal increase over conventional chimney (scenery 2) and 172% increase over closed situation (scenery 1). In this situation, 53.3% of the total air flow removed ($\dot{m}_{3,d}^*$) is originating from the upper inlet.

6. CONCLUSION

In this work, the viability of using both upper and bottom inlets in a solar chimney was verified. The main aspects found were:

- The existence of an upper inlet, by itself, promotes an increase in the chimney's total air flow over a conventional chimney layout.
- With the chimney tested, the simple act of setting the obstruction gap to 5 mm, increased total air flow in 10%, while 53.3% of the total air flow removed by chimney, was taken from the upper inlet.
- Total air flow is highly influenced by obstruction gap dimension, on which, lower is better (valid for scenery 3).
- Insulator gap had a negative effect over the total air flow removed from chimney, mainly due to a decrease in the upper inlet air flow.
- For lower ratios of GAPo/GAPi, the proposed chimney can remove a higher air flow amount over a small chimney, arranged as scenery 1.

Further works are desirable to analyze the velocity profile inside the chimney, as well as cover other influences such as upper inlet height and angle of obstructions. An energy exchange quantification is also suggested to feed the mathematical equations precisely.

7. ACKNOWLEDGEMENTS

The authors would like to acknowledge CAPES (PROSUP program) for all assistance and financial support as well as Contain'it for providing useful materials.

8. REFERENCES

- Amori, K.E. and Mohammed, S.W., 2012. "Experimental and numerical studies of solar chimney for natural ventilation in Iraq". *Energy and Buildings*, Vol. 47, pp. 450–457.
- Asadi, S. et al., 2016. "The effect of solar chimney layout on ventilation rate in buildings". *Energy and Buildings*, Vol. 123, pp. 71–78.
- Awbi, H.B., 1994. "Design considerations for naturally ventilated buildings". *Renewable Energy*, Vol. 5, No. 5-8, pp. 1081–1090.
- Bansal, N.K. et al., 2005. "Modeling of window-sized solar chimneys for ventilation". *Building and Environment*, Vol. 40, No. 10, pp. 1302–1308.
- Bansal, N.K., Mathur, R. and Bhandari, M.S., 1993. "Solar chimney for enhanced stack ventilation". *Building and Environment*, Vol. 28, No. 3, pp. 373–377.
- Bassiouny, R. and Korah, N.S.A., 2009. "Effect of solar chimney inclination angle on space flow pattern and ventilation rate". *Energy and Buildings*, Vol. 41, No. 2, pp. 190–196.
- Bassiouny, R. and Koura, N.S.A.A., 2008. "An analytical and numerical study of solar chimney use for room natural ventilation". *Energy and buildings*, Vol. 40, No. 5, pp. 865–873.

- Bouchair, A., 1994. "Solar chimney for promoting cooling ventilation in southern Algeria". *Building Services Engineering Research and Technology*, Vol. 15, No. 2, pp. 81–93.
- Chen, Z.D. et al., 2003. "An experimental investigation of a solar chimney model with uniform wall heat flux". *Building and Environment*, Vol. 38, No. 7, pp. 893–906.
- Gan, G., 1998. "A parametric study of Trombe walls for passive cooling of buildings". *Energy and Buildings*, Vol. 27, No. 1, pp. 37–43.
- Imran, A.A., Jalil, J.M. and Ahmed, S.T., 2015. "Induced flow for ventilation and cooling by a solar chimney". *Renewable Energy*, Vol. 78, pp. 236–244.
- Jing, H., Chen, Z. and Li, A., 2015. "Experimental study of the prediction of the ventilation flow rate through solar chimney with large gap-to-height ratios". *Building and Environment*, Vol. 89, pp. 150–159.
- Khanal, R. and Lei, C., 2011. "Solar chimney-A passive strategy for natural ventilation". *Energy and Buildings*, Vol. 43, No. 8, pp. 1811–1819.
- Khedari, J., Boonsri, B. and Hirunlabh, J., 2000. "Ventilation impact of a solar chimney on indoor temperature fluctuation and air change in a school building". *Energy and Buildings*, Vol. 32, No. 1, pp. 89–93.
- Malta, F.P., Gouveia, J.L.F. and Albuquerque, C., 2014. "A study of a solar chimney to improve comfort inside shipping containers". In *Proceedings of the 27th International Conference on Efficiency, Cost, Optimization, Simulation and Environmental Impact of Energy Systems*. Abo Akademi University, Turki, Finland.
- Malta, F.P., Gouveia, J.L.F. and Albuquerque, C., 2013. "Investigation of natural convection in solar chimney with trapezoidal section to improve comfort inside shipping containers". In *Proceedings of the 22nd International Congress of Mechanical Engineering*. ABCM, Ribeirão Preto.
- Mathur, J., Mathur, S. and Anupma, 2006. "Summer-performance of inclined roof solar chimney for natural ventilation". *Energy and Buildings*, Vol. 38, No. 10, pp. 1156–1163.
- Ong, K.S., 2003. "A mathematical model of a solar chimney". *Renewable Energy*, Vol. 28, No. 7, pp. 1047–1060.
- Sandberg, M., 1999. "Cooling of Building Integrated Photovoltaics by Ventilation Air". In *Proceedings of HybVent Forum '99, First International One-day Forum on Natural and Hybrid Ventilation*, The University of Sydney, Darlington, New South Wales, Australia.
- Sandberg, M. and Moshfegh, B., 1996a. "Investigation of fluid flow and heat transfer in a vertical channel heated from one side by PV elements, part I - Numerical study". *Renewable Energy*, Vol. 8, No. 1-4, pp. 248–253.
- Sandberg, M. and Moshfegh, B., 1996b. "Investigation of fluid flow and heat transfer in a vertical channel heated from one side by PV elements, part II - Experimental study". *Renewable Energy*, Vol. 8, No. 1-4, pp. 254–258.
- Tan, A.Y.K. and Wong, N.H., 2012. "Natural ventilation performance of classroom with solar chimney system". *Energy and Buildings*, Vol. 53, pp. 19–27.
- Villas-Bôas, T.F., Malta, F.P., Gouveia, J.L.F. and Albuquerque, C., 2015. "Study of different configurations of solar chimney to improve comfort inside shipping containers". In *Proceedings of the 23rd International Congress of Mechanical Engineering*. ABCM, Rio de Janeiro.
- Ziskind, G., Dubovsky, V. and Letan, R., 2002. "Ventilation by natural convection of a one-story building". *Energy and Buildings*, Vol. 34, No. 1, pp. 91–102.

9. RESPONSIBILITY NOTICE

The authors are the only responsible for the printed material included in this paper.